Stochastic Analysis of Switching Power Converters via Deterministic SPICE Equivalents

(Article begins on next page)

10 April 2024

Stochastic Analysis of Switching Power Converters via Deterministic SPICE Equivalents

Paolo Manfredi, *Member, IEEE,* Igor S. Stievano, *Senior Member, IEEE,* Flavio G. Canavero, *Fellow, IEEE*

Abstract—This letter addresses the stochastic analysis of non-linear switching power converters via an augmented circuit equivalent and a single deterministic SPICE simulation. The proposed approach is based on the expansion of the constitutive relations of the circuit elements in terms of orthonormal polynomials within the well-established framework of polynomial chaos. The feasibility and strength of the method are demonstrated on a DC-DC boost converter described by either detailed nonlinear components or via its averaged linear circuit. Excellent modeling accuracy as well as remarkable speed-ups compared to traditional sampling-based approaches are achieved.

Index Terms—Circuit simulation, polynomial chaos, SPICE, stochastic circuits, switched mode power supplies.

I. Introduction

Switching power converters constitute a standard supply configuration in many electrical and electronic applications. In critical (e.g., biomedical or vehicular) equipment, serious concerns are raised by stability and reliability under the unavoidable presence of large uncertainty on power electrical components [1]. Typical examples are provided by inductors and electrolytic capacitors, that are affected by non-negligible manufacturing tolerances, nonideal behavior or measurement errors, as well as parasitics, source noise and operating temperature and conditions [2].

Statistical analysis of power switching networks therefore became a hot topic in the past decade [3]–[5]. The high computational inefficiency that affects traditional techniques, like the Monte Carlo (MC) method or possible enhanced variations based e.g. on the design of experiments or similar tools [6], paved the way to more efficient circuit simulation approaches, such as those based on the polynomial chaos (PC) framework (see, e.g., [5], [7], [8] and reference therein). The underlying idea of PC is to represent circuit responses in terms of basis expansions that carry fundamental statistical information. Combination with statistical tests, e.g. the analysis of variance (ANOVA), possibly allows a preliminary screening and selection of the most relevant random parameters [9].

The present contribution extends the results of previously published papers in this field (see [5], [7], [8]), providing a framework for the circuit-level stochastic analysis of both linear and nonlinear circuits via an augmented deterministic equivalent. One of the main achievements is that the resulting

P. Manfredi, I. Stievano and F. Canavero are with the Department of Electronics and Telecommunications, Politecnico di Torino, Corso Duca degli Abruzzi 24, Torino, 10129 Italy (e-mail: paolo.manfredi@polito.it).

equivalent circuit can be readily simulated in standard SPICE-type simulators, thus allowing circuit designers to rely on existing and well-consolidated tools, providing hundreds of device models, rather than requiring the creation of a customized software and the re-development of pertinent library models. A very general framework for the inclusion of nonlinear components is also outlined, as such enabling the analysis not only of linearized average models for power converters, but also of their detailed nonlinear description.

II. Example Test Case

For illustration purposes we focus this letter on the typical DC-DC boost converter shown in Fig. 1. The above example, belonging to a class of switching circuits widely spread in power electronics, offers a representative test case of a closed-loop system involving both linear and strongly nonlinear circuit components, thus allowing to stress the benefits of the proposed methodology and to demonstrate its feasibility and strength.
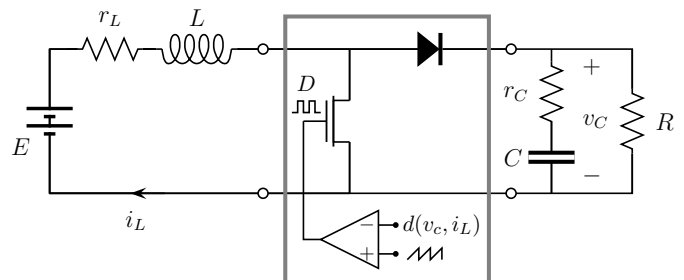

Fig. 1. Example test case: DC-DC boost converter with analog feedback control. The gray box highlights a typical configuration for the nonlinear part of boost circuits, consisting of a switching element, in turn composed by a MOS device and a diode, and of an automatic control, here represented via functional objects.

In Fig. 1, an analog voltage and current feedback control is used. The circuit elements take the following values: $E = 5\,\text{V}$, $r_L = 1\,\text{m}\Omega$, $L = L_0 = 5\,\text{mH}$, $r_C = 5\,\text{m}\Omega$, $C = C_0 = 10\,\mu\text{F}$, whilst the switching frequency is $f_s = 45\,\text{kHz}$. As to the feedback network, the configuration in [3] is considered among a number of existing alternative control strategies. The MOS device is driven by a square wave with a suitable duty-cycle D, that is provided by the feedback network as a function of v_C and i_L. Specifically, the MOS gate control is the output of a comparator, whose non-inverting input is fed by a saw-tooth waveform, whereas its inverting input is defined as $d(v_C, i_L) = V_\text{ref} - k_1 i_L - k_2 v_C$. The coefficients k_1 and k_2 are designed to optimize the performance of the closed-loop circuit and V_ref is the desired output voltage. Here $V_\text{ref} = 12\,\text{V}$,

$k_1 = -0.02\,\Omega$, $k_2 = 0.01$. For additional details, the reader should refer to [3].

When a fine detail of the switching response is not required, the nonlinear part can be replaced by a linear equivalent, which emulates the average behavior of the circuit: an accurate description of the response fluctuation due to the switching elements is lost, but the simulation is much faster. Without loss of generality, the model proposed in [10] is here adopted.

As an example, Fig. 2 shows the time-domain response of the output voltage $v_C(t)$ computed by means of SPICE for two models of the switching network: the curve labeled "full" considers a detailed description of a power MOSFET and a basic diode model; the curve labeled "average" is obtained by considering the linearized average model instead. The simulation is carried out with null initial conditions for the voltage across the capacitor and the current through the inductor. Also, to highlight the effects of unavoidable changes in the load current absorption, the load resistor R is varied every 5 ms and takes the values $20\,\Omega$, $40\,\Omega$ and $30\,\Omega$.
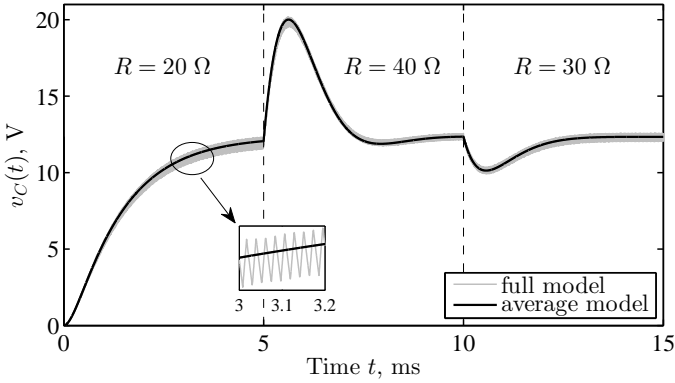

Fig. 2. Transient SPICE simulation of the boost circuit in Fig. 1. Gray line: detailed simulation; black line: simplified average simulation.

In order to illustrate and validate the benefits of the proposed technique, a variability of the dynamical elements L and C will be considered and parameterized as $L = L_0(1 + \sigma_1\xi_1)$ and $C = C_0(1 + \sigma_2\xi_2)$, respectively, where ξ_1 and ξ_2 are independent Gaussian random variables with zero mean and unit variance, whereas σ_1 and σ_2 are the normalized standard deviations. The next section discusses how the SPICE simulation models can be suitably modified to account for the effects of variability on linear and nonlinear circuit components.

III. Polynomial Chaos-Based SPICE equivalents

This section summarizes the basic mathematical tools that allow to create SPICE-compatible circuit models accounting for the variability of network elements. For conciseness, the discussion is based on one random variable only, parameterized by the normalized variable $\xi = \xi_1$, being the extension to the multivariate case straightforward and available in the literature (e.g., see [8]). In presence of such a random quantity, both the voltages and the currents in the network inherently depend on ξ, thus becoming stochastic variables themselves.

The idea underlying the PC is the expansion of the above electrical variables in terms of polynomials, e.g.

$$v(t, \xi) \approx \sum_{k=0}^{P} v_k(t)\varphi_k(\xi), \qquad (1)$$

where P is the number of terms defining the truncated series and $v_k(t)$ are deterministic coefficients to be determined for the nodal or branch voltages. A similar reasoning applies to the circuit currents $i(t)$. Finally, φ_k are the elements of a polynomial basis orthonormal with respect to the inner product:

$$\langle f, g \rangle = \int_{\Re} f(\xi)g(\xi)w(\xi)d\xi, \qquad (2)$$

where $w(\xi)$ is the probability distribution of ξ. According to the Wiener-Askey scheme, for standard distributions, the *orthogonal* polynomials are well-known and correspond to Hermite polynomials for Gaussian random variables, Legendre polynomials for uniform variables, etc. [?]. In order to preserve symmetry and reciprocity in the models, such orthogonal polynomials are normalized so that $\langle \varphi_k, \varphi_j \rangle = \delta_{kj}$ (Kroneker's delta). For instance, the *orthonormal* Hermite polynomials are $\varphi_0 = 1$, $\varphi_1 = \xi$, and $\varphi_2 = \frac{1}{\sqrt{2}}(\xi^2 - 1)$, etc.

The main advantage of the PC representation (1) is that, once the unknown coefficients $v_k(t)$ are computed, the statistical information of $v(t)$ (e.g., its mean or standard deviation) can be effectively computed form (1) via analytical or numerical techniques [7], [8].

The rationale of the proposed simulation approach is to derive deterministic constitutive equations relating the voltage and current coefficients for the circuit elements exhibiting variability. Such relationships are then implemented and simulated in SPICE via equivalent circuits to retrieve the sought-for PC variables. The remainder of this section illustrates the approach by focusing on the derivation of the augmented constitutive equations for two different types of lumped circuit elements: linear and nonlinear.
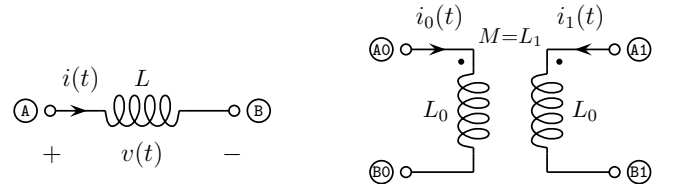

Fig. 3. Linear inductor and its corresponding augmented model.

The first example deals with a linear inductor connecting nodes A and B, and whose characteristic is $v_A(t) - v_B(t) = L\frac{d}{dt}i(t)$, where $v_A(t)$ and $v_B(t)$ are the pertinent nodal voltages and $i(t)$ is the current flowing through the inductor (see the left panel of Fig. 3). For conciseness, all the electrical variables are expressed in terms of a two-term expansion, leading to

$$(v_{A0}(t)\varphi_0 + v_{A1}(t)\varphi_1) - (v_{B0}(t)\varphi_0 + v_{B1}\varphi_1) = \\ = (L_0\varphi_0 + L_1\varphi_1)\frac{d}{dt}(i_0(t)\varphi_0 + i_1(t)\varphi_1)) \qquad (3)$$

The projection of (3) onto the first polynomial φ_0 via (2) produces:

$$v_{A0}\langle\varphi_0, \varphi_0\rangle + v_{A1}\langle\varphi_1, \varphi_0\rangle - v_{B0}\langle\varphi_0, \varphi_0\rangle - v_{B1}\langle\varphi_1, \varphi_0\rangle = \\ = L_0\langle\varphi_0\varphi_0, \varphi_0\rangle\frac{d}{dt}i_0 + L_0\langle\varphi_0\varphi_1, \varphi_0\rangle\frac{d}{dt}i_1 + \\ + L_1\langle\varphi_1\varphi_0, \varphi_0\rangle\frac{d}{dt}i_0 + L_1\langle\varphi_1\varphi_1, \varphi_0\rangle\frac{d}{dt}i_1, \qquad (4)$$

where the dependence on the time variable t is neglected for brevity of notation and the terms $\langle \cdot, \cdot \rangle$ reduce to mere real numbers that can be analytically computed from (2).

The above equation, along with the projection of (3) onto the second polynomial φ_1, leads to the following constitutive relations for the expansion coefficients of the stochastic inductor:

$$\begin{cases} v_{A0}(t) - v_{B0}(t) = L_0 \frac{d}{dt} i_0(t) + L_1 \frac{d}{dt} i_1(t) \\ v_{A1}(t) - v_{B1}(t) = L_1 \frac{d}{dt} i_0(t) + L_0 \frac{d}{dt} i_1(t). \end{cases} \quad (5)$$

It is worthwhile noting that (5) are deterministic because the dependence on the random variable ξ has been suppressed by the projection procedure. This suggests to represent the inductor in terms of a new multi-terminal circuit element involving the coefficients of the node voltages and branch currents. According to (5), this turns out to be a mutual inductor, as illustrated in Fig. 3. The above interpretation also provides a clever way to implement this new element in any SPICE-type simulator by means of standard circuit elements, as follows:

```
.subckt Laugmented A0 B0 A1 B1 PL0=... PL1=...
  L1 A0 B0 PL0
  L2 A1 B1 PL0
  K12 L1 L2 K='PL1/PL0'
.ends Laugmented
```

The approach is readily extended to expansions with a larger number of terms as well as to the modeling of the stochastic capacitor or other linear elements.

The second example involves a circuit element with nonlinear characteristic. For instance, the input-output characteristic of the comparator of Fig. 1 can be expressed as $v_B(t) = F(v_A(t))$, with $F(\cdot)$ being a suitable (e.g., piecewise) nonlinear function, whereas v_A and v_B are the input and output (differential) voltages of the comparator, respectively. Again, a second-order expansion of the electrical variables leads to:

$$v_{B0}(t)\varphi_0 + v_{B1}(t)\varphi_1 = F(v_{A0}(t)\varphi_0 + v_{A1}(t)\varphi_1). \quad (6)$$

The projection of (6) onto the first orthonormal polynomial φ_0 yields:

$$v_{B0}(t) = \int_{\Re} F(v_{A0}(t)\varphi_0(\xi) + v_{A1}(t)\varphi_1(\xi)) \, \varphi_0(\xi)w(\xi)d\xi. \quad (7)$$

The inner product integral on the right-hand side has been made explicit to highlight that, due to the nonlinearity, no closed-form expression is available. In order to arrive at a deterministic and closed-form expression, the integral in (7) is approximated by means of a quadrature rule, thus leading to:

$$v_{B0}(t) \approx \sum_{q=1}^{Q} F(v_{A0}(t)\varphi_0(\xi_q) + v_{A1}(t)\varphi_1(\xi_q)) \, \varphi_0(\xi_q)w_q. \quad (8)$$

In (8), Q is the number of quadrature points ξ_q, and w_q are the corresponding weights, depending on the adopted quadrature rule. It is important to note that (8) is a deterministic nonlinear function, since the terms $\varphi_0(\xi_q)$, $\varphi_1(\xi_q)$ and w_q become numerical coefficients. Moreover, a very good modeling accuracy with a low number of points Q

can be achieved by selecting the optimal Gaussian quadrature rule according to the weighting function $w(\xi)$ (e.g., Gauss-Hermite, Gauss-Legendre, etc.). For Gaussian variability, a Gauss-Hermite quadrature with $Q = 3$ yields for instance $\xi_q = \{-\sqrt{3}, 0, +\sqrt{3}\}$ and $w_q = \{1/6, 4/6, 1/6\}$.

Repeating the procedure for the second polynomial φ_1 provides the sought-for deterministic constitutive equations for the coefficients of the electrical variables. Expressions like (8) are implemented into SPICE by means of standard controlled sources. Also, analogous steps can be readily applied to elements described by a current-voltage characteristic, like diodes, as well as to more complex, possibly multi-terminal, subcircuits, like those modeling MOSFET devices. Fig. 4 provides an illustrative and graphical summary of the proposed method for the general case of a nonlinear multi-terminal device.

The above procedure is applied in an automated fashion to all the linear and nonlinear circuit elements of the stochastic network, and a new augmented circuit is built by suitably interconnecting the augmented counterparts of each element. What is more important, a single deterministic SPICE simulation of the created network allows to compute all the voltage and current coefficients, and subsequently retrieve the statistical information of the circuit response. The proposed procedure does not require dedicated or customized tools for the circuit simulation, thus relying on commercially available SPICE simulators.
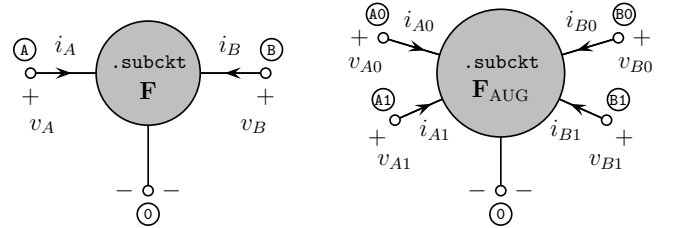

Fig. 4. Graphical interpretation of the expected augmented characteristic of a generic multi-terminal circuit element represented as a subcircuit and possibly representing the MOS device or the comparator in the circuit of Fig. 1.

IV. NUMERICAL RESULTS

This section collects the results of the stochastic simulation of the example test case of Fig. 1. Fig. 5 shows the stochastic simulation of the averaged circuit for the boost converter, carried out with HSPICE by considering $\sigma_1 = \sigma_2 = 5\%$. The gray area results from the superposition of a limited set of MC responses and provides a qualitative idea of the response fluctuation due to circuit uncertainties. The black lines are the average response and the $\pm 3\sigma$ limits estimated using 1000 MC samples. Finally, the markers indicate the same statistical information achieved via the PC-based simulation of the augmented circuit, constructed considering $P = 5$. From the above comparison, a very good accuracy is established for the proposed technique.

To validate the modeling of nonlinear components, a stochastic simulation is performed also for the complete circuit with the MOSFET switch, the diode and the feedback network. In order to provide a thorough comparison on the detailed
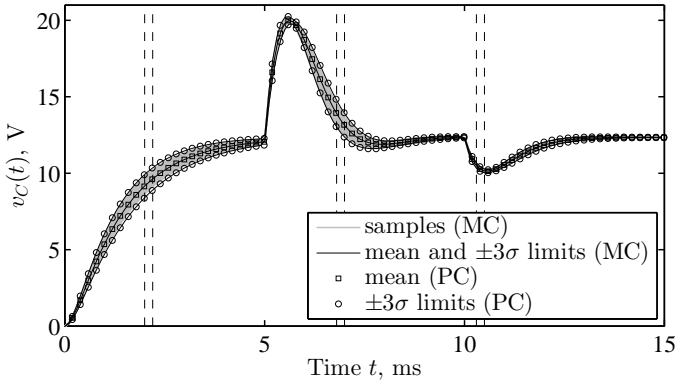
Fig. 5. Stochastic simulation of the averaged circuit. Gray area: fluctuation of the response due to circuit uncertainties; black lines: mean and $\pm 3\sigma$ bounds estimated with 1000 MC samples; markers: mean ($\square$) and $\pm 3\sigma$ bounds ($\circ$) obtained via the PC-based simulation.

switching response, three zoom-ins are shown in Fig. 6. The plots refer to the three time windows indicated by the vertical dashed lines on the averaged response in Fig. 5. The axes and curve labels are the same as in Fig. 5. The statistical information extracted from 1000 MC simulations of the complete nonlinear network is here compared against the PC-based simulation (again with $P = 5$) with the inclusion of augmented nonlinear device models. Excellent accuracy can be again appreciated. For this configuration, the 1000-run MC analysis took 5 h and 19 min, whereas the PC approach required 6 min and 7 s, thus yielding a remarkable speed-up of $52\times$.
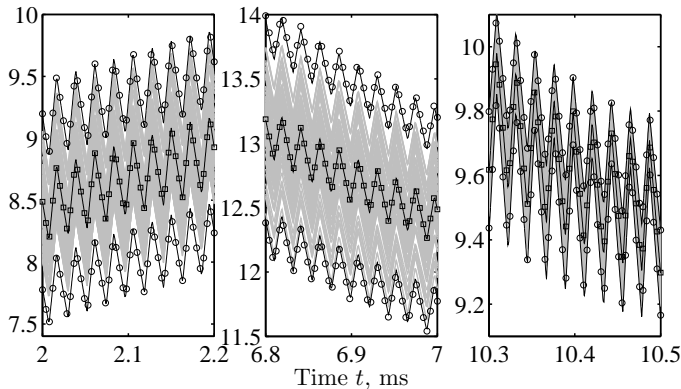

Fig. 6. Stochastic simulation of the complete nonlinear network. The close-ups for three time windows (indicated by vertical dashed lines in Fig. 5) are shown in order to better appreciate the fine detail of the switching behavior. Curve identification is as in the inset of Fig. 5.

Finally, Tab. I shows the relative difference ϵ_σ between the standard deviations of the output voltage at 2.1 ms (i.e., in the middle of the first window in Fig. 6) estimated with PC and MC, the latter using an increasing number of $N = 10$, 100 and 1000 simulation samples. The table indicates that a large number of MC samples is required to approach the PC accuracy. For further information on the convergence and accuracy of both MC and PC, the reader is referred to [8]. It is important to point out, however, that the proposed PC-based method still provides an improvement over MC even when smaller numbers of simulation samples are considered.

TABLE I
ACCURACY ASSESSMENT BETWEEN PC AND MC.

	MC ($N = 10$)	MC ($N = 100$)	MC ($N = 1000$)
ϵ_σ	12.00%	4.02%	1.53%

V. CONCLUSIONS

This letter addresses the stochastic circuit simulation of nonlinear switching networks for power electronics by means of deterministic SPICE equivalents. For a given network with circuit elements defined by uncertain coefficients, the voltage and current variables are expressed in terms of a truncated series of orthonormal polynomials of random variables. The coefficients of the above expansion carry fundamental statistical information and are interpreted as deterministic variables of an equivalent augmented circuit. The polynomial chaos tool, possibly combined with quadrature integration schemes, provides a robust framework for the computation of the SPICE equivalents to be used in the augmented network. A single SPICE simulation of the resulting circuit allows to compute the coefficients of the voltage and current variables and therefore their statistical behavior. An example involving the statistical analysis of a either fully nonlinear or averaged and linearized DC-DC boost converter is used to demonstrate the benefits of the proposed technique in terms of both accuracy and efficiency.

REFERENCES

[1] Y. Song and B. Wang, "Survey on reliability of power electronic systems," *IEEE Trans. Power Electron.*, vol. 28, no. 1, pp. 591–604, Jan. 2013.
[2] Y.-S. Roh et al., "A two-phase interleaved power factor correction boost converter with a variation-tolerant phase shifting technique," *IEEE Trans. Power Electron.*, vol. 29, no. 2, pp. 1032–1040, Feb. 2014.
[3] A. Sangswang and C. O. Nwankpa, "Noise characteristics of DC-DC boost converters: experimental validation and performance evaluation," *IEEE Trans. Ind. Electron.*, vol. 51, no. 6, pp. 1297–1304, Dec. 2004.
[4] F.-H. Hsieh, N.-Z. Yen, and Y.-T. Juang, "Optimal controller of a buck DC-DC converter using the uncertain load as stochastic noise," *IEEE Trans. Circuits Syst. II, Exp. Briefs*, vol. 52, no. 2, pp. 77–81, Feb. 2005.
[5] Q. Su and K. Strunz, "Stochastic polynomial-chaos-based average modeling of power electronic systems," *IEEE Trans. Power Electron.*, vol. 26, no. 4, pp. 1167–1171, Apr. 2011.
[6] Q. Zhang et al., "Development of robust interconnect model based on design of experiments and multiobjective optimization," *IEEE Trans. Electron Devices*, vol. 48, no. 9, pp. 1885–1891, Sep. 2001.
[7] Q. Su and K. Strunz, "Stochastic circuit modeling with Hermite polynomial chaos," *IET Electronics Letters*, vol. 41, no. 21, pp. 1163–1163, Oct. 2005.
[8] A. Biondi et al., "Variability analysis of interconnects terminated by general nonlinear loads," *IEEE Trans. Compon. Packag. Manuf. Techol.*, vol. 3, no. 7, pp. 1244–1251, Jul. 2013.
[9] P. Manfredi and F. G. Canavero, "Polynomial chaos-based tolerance analysis of microwave planar guiding structures," *2011 IEEE MTT-S Int. Microwave Symp. Dig.*, pp. 1–4, June 2011.
[10] V. Vorperian, "Simplified analysis of PWM converters using model of PWM switch. Continuous conduction mode," *IEEE Trans. Aerosp. Electron. Syst.*, vol. 26, no. 3, pp. 490–496, May 1990.